

Discordant Results on FeCO Deformability in Heme Proteins Reconciled by Density Functional Theory

Thomas G. Spiro* and Pawel M. Kozlowski

Department of Chemistry, Princeton University
Princeton, New Jersey 08544

Received September 18, 1997

We report density functional theory (DFT) calculations of the heme–Fe–CO distortion energetics and of the direction of the C–O stretching transition dipole, which reconcile apparently conflicting experimental results from X-ray crystallography and infrared dichroism.¹ Although CO binds in a linear fashion to transition metal ions,² the first well-resolved crystal structures of the myoglobin CO adduct, MbCO,^{3,4} revealed a large off-axis distortion, which was attributed to steric interaction with the imidazole ring of a distal histidine residue. Several subsequent structures under different crystallization conditions have given less severe but still significant distortions (Figure 1).^{5–6} However, distorted FeCO is not supported by infrared polarization measurements,^{7,8} which indicate a nearly upright geometry.

Also at issue is the question of steric contributions to the discrimination against CO and in favor of O₂ exhibited by heme proteins. In the absence of protein, the heme group binds CO much more strongly than O₂, by a factor of ca. 30 000, but this factor is reduced to 25–40, depending on the organism, in Mb.⁹ Collman et al.¹⁰ first proposed that this dramatic reduction, without which we would be poisoned by our endogenous CO, is due to the steric hindrance to upright FeCO exerted by the distal histidine. This idea has made its way into textbooks¹¹ but is thrown into question by the results of site-directed mutagenesis,⁹ which show only modest increases in CO affinity when the distal histidine is replaced by other residues, and the increments do not correlate with the size of the side chain.

Skepticism about CO deformability is based on the limited resolution of protein diffraction data¹² and on the strong electronic preference for linear Fe–C–O bonding, based on the importance of Fe/d_π–CO/π* back-bonding to the CO binding energy. Bending of the CO ligand misorients the d_π and π* orbitals, reducing back-bonding.¹³ The large deviations from linearity initially reported, 40–60°,^{3,4} would appear to cost a

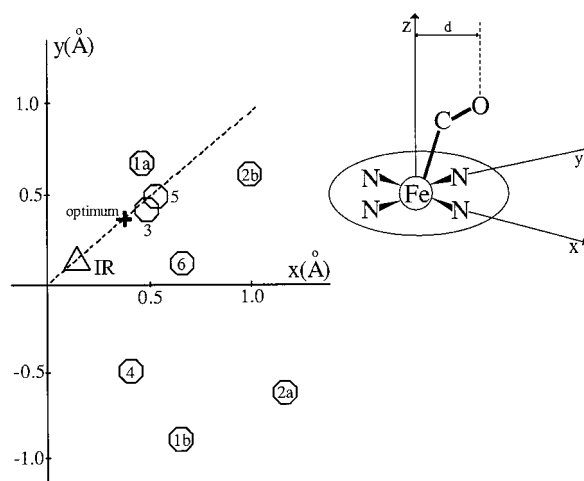


Figure 1. Projection of the O-atom displacement from the heme *z* axis in MbCO crystal structures. Points 1a and 1b: native *P*₂₁ MbCO crystal, PDB file 1mbc.³ Points 2a and 2b: native *P*₂₁ MbCO crystal, PDB file 2mb5.⁴ Point 3: “wild-type” D122N mutant of sperm whale myoglobin that crystallizes in a *P*6 space group, PDB file 2mgk.⁵ Points 4–6: native *P*₂₁ MbCO crystals at pHs 4, 5, and 6, PDB files 1spe, 1vxc, and 1vxf.⁶ (Δ) Calculated position if the CO is at a 6.9° angle to the *z* axis.⁷ (+) Calculated position along the DFT minimum energy distortion coordinate (dotted line) for a 6.9° transition dipole. (Note that the DFT coordinate bisects the Fe–N axes, but the ±45° directions are equivalent.)

prohibitive amount of energy and to be incompatible with CO binding.¹² However, Li and Spiro¹⁴ pointed out that the estimated energy cost diminishes considerably, if multiple distortion coordinates, porphyrin buckling and Fe–C tilting as well as Fe–C–O bending, are permitted in concert. Recently, Ghosh and Bocian¹⁵ have reported an additional reduction in the distortion energy estimate because of a negative interaction force constant between the bending and tilting coordinates, as revealed by DFT calculations. We have now confirmed and extended this result using gradient-corrected DFT (Table 1, see footnote) and full vibrational analysis on an imidazole(heme)CO model (Kozlowski, Vogel, Zgierski, and Spiro, manuscript in preparation). The negative interaction constant reflects cooperativity between the bend and tilt coordinates; they both diminish back-bonding and therefore reinforce one another. Thus bending becomes easier when tilting occurs, and vice versa.

Consequently, it takes less energy to distort the FeCO unit than would be expected from the isolated coordinate force constants. When tilting and bending motions are allowed simultaneously, the potential curve for off-axis displacement becomes quite shallow (Figure 2). A 1.3-Å displacement of the O atom from the heme *z* axis costs 4.8 kcal/mol, while a 0.5-Å displacement costs only 0.7 kcal/mol. This range encompasses all the reported crystal structures (Figure 1).

How then can we understand the infrared polarization and photoselection results, which indicate an essentially upright FeCO unit? While early photoselection experiments^{16,17} suggested substantial distortion, careful reduction of systematic errors led Anfirud and co-workers⁷ to conclude that the C–O direction is within 7° of the heme normal. This outcome supports the single-crystal IR polarization measurements of Champion and Sage and co-workers,⁸ in which the C–O dipole direction relative to the

* To whom correspondence should be addressed.

(1) Spiro, T. G.; Kozlowski, P. M.; *J. Biol. Inorg. Chem.* **1997**, *2*, 516. Sleboznick, C.; Ibers, J. A. *J. Biol. Inorg. Chem.* **1997**, *2*, 521. Vanberg, T.; Bocian, D. F.; Ghosh, A. *J. Biol. Inorg. Chem.* **1997**, *2*, 526. Lim, M.; Jacson, T. A.; Anfirud, P. A. *J. Biol. Inorg. Chem.* **1997**, *2*, 531. Sage, T. J. *J. Biol. Inorg. Chem.* **1997**, *2*, 537. Olson, J. S.; Phillips, G. N., Jr. *J. Biol. Inorg. Chem.* **1997**, *2*, 544.

(2) Peng, S. M.; Ibers, J. A. *J. Am. Chem. Soc.* **1976**, *98*, 8032.

(3) Kuriyan, J.; Wilz, S.; Karplus, M.; Petsko, G. A. *J. Mol. Biol.* **1986**, *192*, 133.

(4) Cheng, X.; Schoenborn, B. *Acta Crystallogr.* **1990**, *B46*, 195; *J. Mol. Biol.* **1991**, *220*, 381. Norvell, J. C.; Nunes, A. C.; Schoenborn, B. *Science* **1975**, *190*, 568. Hanson, J. C.; Schoenborn, B. P. *J. Mol. Biol.* **1981**, *153*, 117.

(5) Quillin, M. L.; Arduini, R. M.; Olson, J. S.; Phillips, G. N., Jr. *J. Mol. Biol.* **1993**, *234*, 140.

(6) Young, F.; Phillips, G. N., Jr. *J. Mol. Biol.* **1996**, *256*, 762.

(7) Lim, M.; Jackson, T. A.; Anfirud, P. A. *Science* **1995**, *269*, 962.

(8) Ivanov, D.; Sage, J. T.; Keim, M.; Powell, J. R.; Asher, S. A.; Champion, P. M. *J. Am. Chem. Soc.* **1994**, *116*, 4139. Sage, J. T. *Appl. Spectrosc.* **1997**, *51*, 568. Sage, J. T.; Jee, W. *J. Mol. Biol.* **1997**, *274*, 21–26.

(9) Springer, B. A.; Sligar, S. G.; Olson, J. S.; Phillips, G. N., Jr. *Chem. Rev.* **1994**, *94*, 699.

(10) Collman, J. P.; Brauman, J. I.; Halbert, T. R.; Suslick, K. S. *Proc. Natl. Acad. Sci. U.S.A.* **1976**, *73*, 3333.

(11) Stryer, L. *Biochemistry*, 3rd ed.; Freeman & Co.: New York, 1988; p 149.

(12) Ray, G. B.; Li, X.-Y.; Ibers, J. A.; Sessler, J. L.; Spiro, T. G. *J. Am. Chem. Soc.* **1994**, *116*, 162.

(13) Hoffman, R.; Chen, M. M. L.; Thorn, D. L. *Inorg. Chem.* **1977**, *16*, 503.

(14) Li, X.-Y.; Spiro, T. G. *J. Am. Chem. Soc.* **1988**, *110*, 6024.

(15) Ghosh, A.; Bocian, D. F. *J. Phys. Chem.* **1996**, *100*, 16.

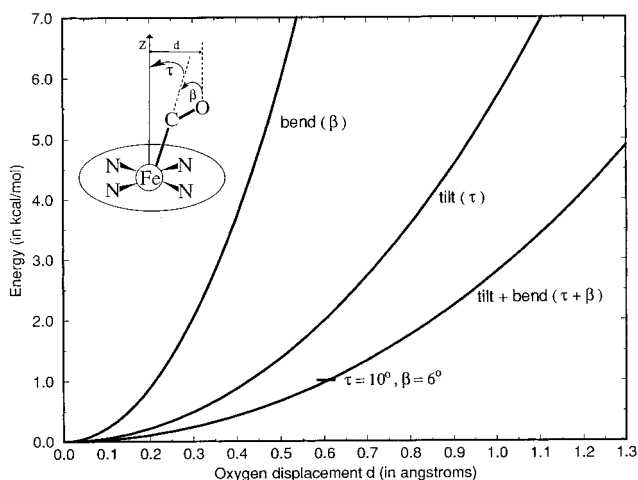
(16) Ormos, P.; Braunstein, D.; Frauenfelder, H.; Hong, M. K.; Lin, S.-L.; Sauke, T. B.; Youn, R. D. *Proc. Natl. Acad. Sci. U.S.A.* **1988**, *85*, 8492.

(17) Moore, J. N.; Hansen, P. A.; Hochstrasser, R. M. *Proc. Natl. Acad. Sci. U.S.A.* **1988**, *85*, 5062.

Table 1. FeCO Bending and Tilting Force Constants^a (mdyn Å/rad²)

	$k_{\beta\beta}$	$k_{\tau\tau}$	$k_{\tau\beta}$
Li and Spiro (empirical ^b)	0.80	0.72	0.0
Ghosh and Bocian (DFT ^c)	0.476	1.054	-0.400
this work (DFT ^d)	0.426	0.661	-0.266

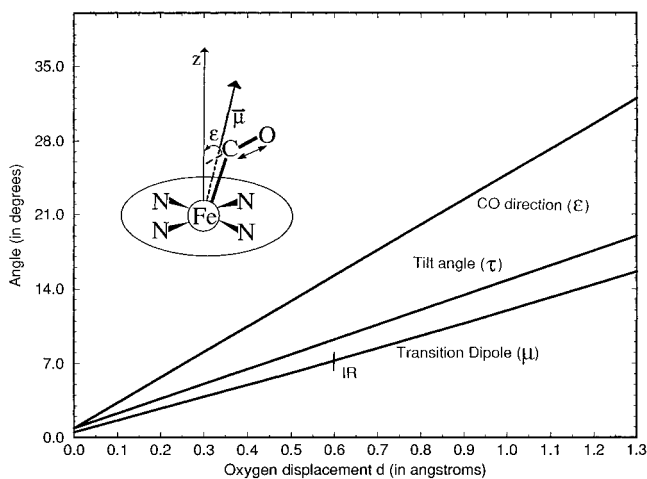
^a $k_{\beta\beta}$ and $k_{\tau\tau}$ are principal bending and tilting constants; $k_{\tau\beta}$ is the bend-tilt interaction constant. ^b From a simplified normal mode calculation.¹⁴ ^c Numerical force constants for an imidazole(Fe^{II} porphyrin)CO model constructed by fitting 15 single-point energies (without geometry optimization) along the bend and tilt coordinates based on the local exchange-correlation functional of Hedin and van Barth.¹⁷ ^d Analytical force constants for an imidazole(Fe^{II} porphyrin)CO model based on gradient-corrected DFT calculations with Becke's three-parameter exchange functional in combination with the Lee, Yang, and Parr (LYP) correlation functional (B3-LYP) as implemented in Gaussian 94 suite of programs for electronic structure calculations.

**Figure 2.** Harmonic energies calculated via DFT for bending alone (β), tilting alone (τ), and a minimum energy combination of bending and tilting.

crystal axes was determined; the angle relative to the heme normal was found to be $6.7 \pm 0.9^\circ$. If the Fe-C and CO bond lengths are the standard 1.79 and 1.14 Å, this angle implies an O-atom displacement of ~ 0.2 Å. While the crystal structures show considerable scatter (Figure 1), they do not include displacements as small as this.

However, both IR methods rest on a crucial but untested assumption, namely that the transition dipole of the C-O stretching IR band is coincident with the C-O bond vector. While this assumption may seem self-evident, it actually is not, as has been pointed out by Jewsbury et al.¹⁸ The Fe d_π electrons are shared with the π^* orbitals on the CO and with the π^* orbitals on the porphyrin ring. The extent of this mutual overlap is illustrated by the fact that the porphyrin ring vibrational frequencies are significantly higher in heme-CO adducts than in adducts with non-back-bonding ligands.¹⁹ The CO draws π^* electron density away from the porphyrin, via the Fe d_π orbitals. Thus, when the C-O bond is stretched, the valence electrons oscillate throughout the molecule. This is why the IR absorptivity is much higher in heme-CO adducts than in unbound CO.²⁰ What consequence does this delocalization have for the transition dipole direction? The dipole will be along the C-O bond as long as the CO is perpendicular to the heme, but the resultant of the electronic oscillations will not necessarily follow the C-O bond once it is distorted.

We investigated this question by calculating the DFT transition dipole direction for various geometries along the minimum energy distortion path (Figure 3) and found that the direction is much closer to the Fe-C bond vector than to the C-O bond vector, even though the normal mode eigenvector is localized along the C-O bond, as expected. When the C-O bond is stretched, the

**Figure 3.** Calculated C-O stretching transition dipole direction (μ) along the DFT minimum energy distortion path.

electrons mainly oscillate along the Fe-C bond, reflecting the importance of back-bonding. The IR methods measure an angle somewhat less than the Fe-C tilt, not the overall CO distortion.

Using the 6.9° transition dipole, we calculate a minimum energy structure with $\tau = 9.5^\circ$ and $\beta = 5.8^\circ$ (see Figure 3). The O-atom displacement is ~ 0.6 Å, which falls within the crystallographic distribution (Figure 1). Thus there is no conflict between the IR and crystallographic measurements. The broad distribution of crystallographic positions is consistent with a shallow potential energy curve and a small distortion energy. The DFT calculation gives ~ 1.0 kcal/mol for the distortion energy.

This value is consistent with the results of binding studies on site mutants of Mb.^{5,9,21} In almost all cases replacement of the distal histidine, H64 (for sperm whale Mb), increased the CO affinity, consistent with an inhibitory role for H64. The biggest effect was observed for the leucine mutation, H64L, which raised the CO affinity by 1.6 kcal/mol.⁹ Crystallography shows the leucine side chain to be undisturbed by CO binding,⁵ whereas the histidine side chain is significantly displaced in the wild-type protein.^{3,4} In addition, a water molecule which is H-bonded to the distal residue in the wild-type deoxyMb is absent in deoxy H64L.⁵ Thus 1.6 kcal/mol is the distal histidine distortion energy plus its electronic interaction energy with the bound CO, which has been estimated at roughly 0.5 kcal/mol,¹² minus the energy for displacement of the distal water molecule in deoxyMb. A distortion energy on the order of 1 kcal/mol is therefore not unreasonable. Thus about 25% of the 4.0 kcal/mol discrimination against CO is attributable to the steric hindrance by the distal histidine.

The remaining 75% can be attributed to the electronic attraction of the distal histidine to the bound O₂, which results in a well-defined H bond.²³ This attraction is much greater than for bound CO because the extent of electron transfer from Fe[II] to the bound ligand is much greater for O₂.²⁴ Consistent with this interpretation, the H64L mutation lowers the O₂ affinity by 2.3 kcal/mol,⁹ which, together with the 1.6 kcal/mol increase in CO binding energy, completely abolishes the CO/O₂ discrimination of the wild-type protein.

JA9732946

(18) Jewsbury, P.; Yamamoto, S.; Minato, T.; Saito, M.; Kitagawa, T. *J. Phys. Chem.* **1995**, *99*, 12677.

(19) Spiro, T. G.; Burke, J. M. *J. Am. Chem. Soc.* **1976**, *98*, 5482.

(20) Lim, M.; Jacson, T. A.; Anfirud, P. A.; *Nat. Struct. Biol.* **1997**, *4*, 209.

(21) Li, T.; Quillin, M. L.; Phillips, G. N. Jr.; Olson, J. S. *Biochemistry* **1994**, *33*, 1433.

(22) Jameson, G. B.; Molinaro, F. S.; Ibers, J. A.; Colleman, J. P.; Brauman, J. I.; Rose, E.; Suslick, K. S. *J. Am. Chem. Soc.* **1980**, *102*, 3244.

(23) Phillips, S. E. V.; Schoenbron, B. P. *Nature* **1981**, *292*, 81.

(24) Weiss, J. J. *Nature (London)* **1964**, *202*, 83.